

Making 802.11 DCF Optimal: Design, Implementation, and Evaluation

Jinsung Lee,
Yung Yi, Song Chong
EE Dept., KAIST
Daejeon, Korea

Bruno Nardelli,
Edward W. Knightly
ECE Dept., Rice Univ.
Houston, TX, USA

Mung Chiang
EE Dept. Princeton Univ.
Princeton, NJ, USA

ABSTRACT

This paper proposes a new protocol called *Optimal DCF* (O-DCF). Inspired by a sequence of analytic results, O-DCF modifies the rule of adapting CSMA parameters, such as backoff time and transmission length, based on a function of the demand-supply differential of link capacity captured by the local queue length. Unlike clean-slate design, O-DCF is fully compatible with 802.11 hardware, so that it can be easily implemented only with a simple device driver update. Through extensive simulations and real experiments with a 16-node wireless network testbed, we evaluate the performance of O-DCF and show that it achieves near-optimality, and outperforms other competitive ones, such as 802.11 DCF, optimal CSMA, and DiffQ in a wide range of scenarios.

1. INTRODUCTION

Extensive research documents inefficiency and unfairness of the standard 802.11 DCF and suggests ways to improve it. Some proposals take a clean-slate approach to redesign CSMA. Optimality in performance can sometimes be proved under idealized assumptions such as no collision or perfect synchronization. Other proposals are constrained by operating over legacy 802.11 hardware with only a device driver update, but are often unable to attain optimality. In this paper, we propose a new protocol, called *Optimal DCF* (O-DCF), which demonstrates that a collection of design ideas can be effectively combined to transform legacy 802.11 DCF into a near-optimal yet also practical protocol.

Among prior methods to improve 802.11 DCF is the seemingly conflicting pair of random access philosophies: in face of collisions, should transmitters become more aggressive given that the supply of service rate may become lower than the demand (as in the recently developed theory of Optimal CSMA (oCSMA), e.g., [15, 22, 23, 25, 27])? Or should they become less aggressive given that collisions signal a contentious RF environment (as in a typical exponential backoff in today's 802.11 DCF)? We show that these two conflicting approaches are in fact complementary. The best combination depends on the logical contention topology, but can be learned without knowing the topology.

As developed in theory such as oCSMA, a product of

access probability, which is determined by contention window (CW) in the backoff, and transmission length should be proportional to the supply-demand differential for long-term throughput fairness. Towards the goal of achieving high performance in practice, a good combination of access probability and transmission length is taken, where such a good access probability is “searched” by Binary Exponential Backoff (BEB) in a fully distributed manner to adapt to the contention levels in the neighborhood, and then transmission length is suitably selected for long-term throughput fairness. Thus, BEB is exploited not just to conservatively respond to temporal collisions, as in standard 802.11, but also to be adapted to appropriate access aggressiveness for high long-term fairness and throughput by being coupled with the transmission length.

We first summarize three key design ideas of O-DCF:

- D1.** Link access aggressiveness is controlled by both CW size and transmission length, based on per-neighbor local queue length at MAC layer, where the queue length quantifies supply-demand differential. Links with bigger differential (i.e., more queue buildup) are prioritized in media access by decreasing CW size and/or increasing transmission length.
- D2.** The CW size and transmission length are adapted in a fully distributed manner, depending on network topology affecting contention patterns in the neighborhood. Each link chooses the initial CW size as a decreasing function of the local queue length and then increases the CW size against collisions (i.e., backoff). Transmission length is set proportional to some product of the CW size (at which transmission succeeds) and the local queue length.
- D3.** When wireless channels are heterogeneous across links, e.g., a link with 2Mbps and another link with 6Mbps, the link capacity information is reflected in controlling access aggressiveness by scaling the queue length proportionally to the link capacity. This adaptive control based on link capacity ensures better fairness and higher throughput, since links with better channel condition are scheduled more than those with poor channel condition.

In *D2*, for the case when nodes can sense each other and contends symmetrically, the CW size is appropriately chosen to be a reasonably low value to reduce collisions, and then the transmission length is chosen to be a function of queue length. For the topology called flow-in-the-middle (FIM)¹ where inner and outer links have different contention degrees (i.e., asymmetric contention), the CW size of a link that experiences more contention is adjusted to be smaller than those of other links with less contention, so that it can get enough transmission chances and thus fairness is ensured. We will show that this selective control of CSMA parameters works well even in challenging topologies in which 802.11 DCF yields severe performance degradation, such as hidden terminal (HT), information asymmetry (IA), FIM, and packet capture.

The key design ideas mentioned above are implemented through the following protocol mechanisms:

- P1.** Each transmitter maintains two queues for each neighbor, referred to as Control Queue (CQ) and Media Access Queue (MAQ). CQ buffers the packets from the upper-layer which are to be dequeued into MAQ. The size of MAQ refers to the local queue length in *D2*, determining access aggressiveness by adjusting CW size and transmission length. The dequeue rate from CQ to MAQ is appropriately controlled to ensure (proportional) fairness and high throughput.
- P2.** Once the initial CW size is chosen as a function of the size of MAQ, BEB “searches” for the CW size at which transmission becomes successful in a fully distributed manner. This successful CW size is used to choose the transmission length as described in *D2*.
- P3.** We adapt transmission length based on time rather than bytes to achieve time fairness under heterogeneous channels. To that end, we exploit information from the rate-adaptation module in the 802.11 driver to determine the proper number of bytes to send, according to modulation and coding rate in use.

All of the above mechanisms can be implemented using unmodified 802.11 chips, as we have done in evaluating O-DCF over a 16-node wireless testbed. In particular, the mechanisms satisfy the following constraints of staying within 802.11:

- C1. Interface queue (IQ).** 802.11 hardware has a FIFO queue for storing packets ready for actual transmission to the media such that neighbor-specific packet control such as CQ and MAQ necessitates additional queues on top of IQ.
- C2. CW granularity.** CW values are allowed by only some powers of two and thus we can only choose the value from the set $\{2^n - 1, n = 1, \dots, 10\}$.
- C3. BEB.** BEB (in which CW doubles for each collision up to a maximum value) is often hard-coded and cannot be nullified by software control. Also, once BEB is started,

a typical device driver, e.g., MadWiFi [2], does not allow the driver to read the CW size at which the transmission is successful.

- C4. Maximum aggregate frame size.** The packet size is bounded by a value that depends on the 802.11 chipset. For chipsets supporting packet aggregation, the packet size is constrained by a maximum aggregation size, e.g., 64 KB in 802.11n [31]. Otherwise, it is constrained by a much shorter size, e.g., 2304 B in 802.11a/b/g.

To evaluate the performance of O-DCF, we have implemented O-DCF on a wireless testbed with 16 nodes as well as simulator for large-scale scenarios that are difficult to be configured in the real testbed. By comparing O-DCF with 802.11 DCF, two versions of oCSMA, and DiffQ [34], we observe that in presence of conditions that are known to be critical to other CSMA protocols, O-DCF achieves near-optimal throughput, fairly distributed among flows, with up to 87.1% fairness gain over 802.11 DCF while keeping high network utility in our experiments.

2. RELATED WORK

Problems and Enhancements of 802.11. Numerous papers have reported the performance problems of 802.11 DCF, and proposed many solutions to them. To name just a few, 802.11 DCF has severe performance degradation and throughput disparities among contending flows in the topologies such as HT, IA, FIM, and packet capture [4, 9, 11, 33], and heterogeneous link capacities [12]. We classify the solution proposals into the efforts of MAC and PHY layers. Some papers proposed new access methods such as dynamic adjustment of CW under 802.11 DCF, e.g., [7, 13] and there exist the implementation researches along this line, e.g., [10, 30]. Other work presented efficient aggregation schemes and their real implementations for improving throughput, e.g., [16, 17]. Note that most implementations mentioned above individually focused on some specific topologies such as fully-connected (FC) case, and do not explicitly consider problematic ones such as HT, IA, and FIM. With the aid of PHY-layer, there are totally novel approaches, e.g., [21, 28]. This kind of work exploits more information from PHY layer and/or applies new PHY technologies other than CSMA. In O-DCF, we extend MAC-level approach by controlling the CW size as well as the transmission length based on the demand-supply differential, thus yielding more performance benefit over 802.11 DCF. The PHY-layer based approach is somewhat orthogonal to our approach, which even can be integrated with O-DCF for further performance improvement.

Optimal CSMA. Recently, analytical studies proved that, under certain assumptions, queue-length based scheduling via CSMA can achieve maximum throughput without message passing e.g., [15, 22, 27], which is referred to as oCSMA in this paper. Furthermore, multiple theoretical work presented solutions based on the similar mathematical framework, each of them focusing on different aspects of the protocol operation [6, 23, 25, 26]. Our work is in part motivated

¹Throughout this paper, we use ‘flow’ and ‘link’ interchangeably.

by oCSMA theory, but as reported in [20, 24] and our evaluation, there still exist many gaps between oCSMA theory and 802.11 practice.

Implementation of queue based CSMA. A limited number of work on the implementation of oCSMA exists, mainly with focus on evaluation [20, 24]. They show that multiple adverse factors of practical occurrence not captured by the assumptions behind the theory can hinder the operation of oCSMA, introducing severe performance degradation in some cases [19, 24]. Other work is devoted to bridge the gaps between theory and practice by reflecting queue length over 802.11 [3, 18, 34]. In [34], the authors implemented a heuristic differential backlog algorithm (DiffQ) over 802.11e. EZ-Flow was proposed to solve instability due to large queue build-ups in 802.11 mesh networks [3]. Very recently, the authors in [18] implemented a backpressure scheduling based on TDMA MAC, which operates in a centralized way.

3. HOW DOES O-DCF WORK?

We start by listing four key elements in O-DCF.

- (i) *Section 3.1.* Each transmitter is equipped with two queues for each neighbor, CQ and MAQ. CQ is a buffer to store the packets from the upper-layer and its dequeue rate into MAQ is controlled by a certain rule in strict relation to proportional fairness.
- (ii) *Section 3.2.* The size of MAQ, which quantifies the differential between demand and supply, is used to control the link access aggressiveness by adjusting CW size and transmission length. First, the initial CW size is determined by a sigmoid function of the size of MAQ, and then BEB is applied for collisions. Thus, the link is prioritized when the demand-supply differential becomes large.
- (iii) *Section 3.3.* The transmission length of each link is determined by the product of the success CW size, i.e., the CW size at which transmission succeeds, and MAQ size. Typically, the success CW size is often hard to know from the device driver, thus we employ a method of estimating the success CW size.
- (iv) *Section 3.4.* Channel heterogeneity is reflected by scaling the MAQ size by the link capacity. This gives more priority to the links with better channel conditions in media access, ensuring more efficient rate allocation in terms of time fairness.

3.1 Supply-Demand Differential

In 802.11 DCF, the packets from the upper-layer are enqueued to IQ at the 802.11 chip for media access. In O-DCF, we maintain two per-neighbor queues (CQ and MAQ) over IQ (due to *CI*), to balance the link's supply and demand through fair media access, as shown in Figure 1. Denote by $Q_l^C(t)$ and $Q_l^M(t)$ the sizes of CQ and MAQ for each link l at time t . We further maintain a variable $q_l^M(t)$, which is simply the scaled version of $Q_l^M(t)$, i.e., $q_l^M(t) = bQ_l^M(t)$, where b is some small value, say 0.01. The value of $Q_l^M(t)$

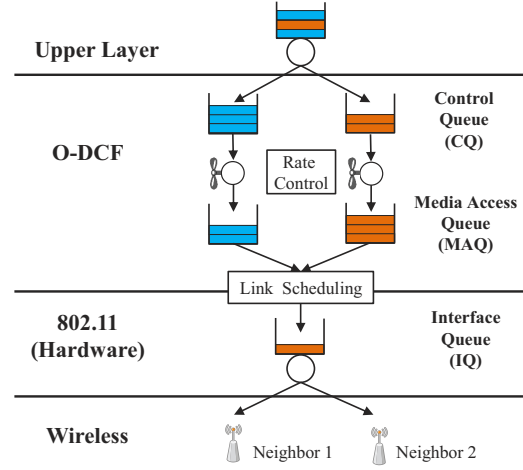


Figure 1: Queue structure of O-DCF.

is crucial in O-DCF in that both the dequeue rate from CQ to MAQ and the aggressiveness of media access tightly rely on $Q_l^M(t)$.

First, we control the dequeue rate from CQ to MAQ (when CQ is non-empty), such that it is inversely proportional to $q_l^M(t)$, by $V/q_l^M(t)$, where V is some constant controlling the sensitivity of the dequeue rate to MAQ. Second, in terms of aggressiveness in media access, an initial CW size and transmission length, which determine the dequeue rate of MAQ, is set as a function of $q_l^M(t)$ (see Sections 3.2 and 3.3 for details). Then, whenever a new arrival from CQ or a service (i.e., packet transmission) from successful media access occurs, $Q_l^M(t)$ is updated by:

$$Q_l^M(t + \delta t) = \left[Q_l^M(t) + (\text{arrival from CQ} - \text{service from MAQ}) \right] \begin{matrix} Q_{\max} \\ Q_{\min} \end{matrix}, \quad (1)$$

where δt is the elapsed time of the next arrival or service event after t . The service from MAQ occurs when the HOL (Head-Of-Line) packet of MAQ is moved into IQ. For multiple neighbors, the largest MAQ is served first; If the chosen transmission length exceeds the maximum aggregation size, multiple packets from the same MAQ are scheduled in succession. Q_{\max} is the physical buffer limit of MAQ, but Q_{\min} is set by us as some positive value to prevent too severe oscillations of $Q_l^M(t)$, where too small Q_{\min} would sometimes lead to impractically high injection rate from CQ to MAQ, when $Q_l^M(t)$ (and thus $q_l^M(t)$) approaches zero, where recall that the injection rate is $V/q_l^M(t)$.

3.2 Initial CW with BEB

When a link l is scheduled at time t , its initial CW size ($CW_l(t)$) and the number of bytes to transmit ($\mu(t)$) are set adaptively as a function of the size of MAQ. First, $\mu(t)$ -byte

transmission over l is assigned with the following CW size:

$$CW_l(t) = \frac{2(\exp(q_l^M(t)) + C)}{\exp(q_l^M(t))} - 1, \quad (2)$$

where C is some constant whose suitable value will be discussed later. We want to use $CW_l(t)$ as the minimum CW (CW_{\min}) in 802.11 DCF, but due to the constraint **C2** that 802.11 hardware only allows CW values as powers of two, we use one of possible values closest to (2) as CW_{\min} . Then, the media access is attempted after the time (in mini-slots) randomly chosen from the interval $[0, CW_{\min}]$. Intuitively, we assign higher aggressiveness in media access for larger MAQ size, remarking that (2) is decreasing with $q_l^M(t)$. Whenever collision happens, this CW value exponentially increases by BEB from **C3**. We will discuss later that BEB is not just an inevitable component due to our design constraint of the 802.11 legacy hardware, but is also an important component to improve performance inside our design rationale.

It is often convenient to interpret CW_l with its corresponding access probability p_l using the relation $p_l = 2/(CW_l + 1)$ [7, 13], where the initial CW_l selection in (2) is regarded as the following *sigmoid* function:

$$p_l(t) = \frac{\exp(q_l^M(t))}{\exp(q_l^M(t)) + C}. \quad (3)$$

We delay our discussion on why and how this sigmoidal type function helps and what choice of C is appropriate to Section 4.2.3.

3.3 Transmission Length Selection

Our design on selecting transmission length $\mu_l(t)$ whenever the media is grabbed by link l is to set $\mu_l(t)$ as a function of the success access probability (equivalently, the success CW size) and the size of MAQ (i.e., $Q_l^M(t)$). Again, by the success CW size, we mean that the transmission becomes successful at that CW size, which is often larger than the initial CW size due to BEB. The rationale to search for the success CW size lies in the fact that it is the actual value used in media access for successful transmission. However, such a success CW size is often hard to be read by the device driver (**C3**). Therefore, we estimate it based on the equation [35] which discloses the connection between the initial CW (CW_l), collision ratio (p_c) and the success access probability after BEB (denoted by \tilde{p}_l), given by:

$$\tilde{p}_l = \frac{2q(1 - p_c^{m+1})}{(CW_l + 1)(1 - (2p_c)^{m+1})(1 - p_c) + q(1 - p_c^{m+1})}, \quad (4)$$

where $q = 1 - 2p_c$ and m is the maximum retransmission limit. The value of p_c can be computed for arbitrary topologies [9], if nodes have the complete knowledge of topology via message passing which is often expensive. To know p_c without such message passing, we approximate p_c by measuring the packet collisions over the last t' seconds (say one second) and averaging them. The measurement on p_c is

based on counting the unacknowledged number of transmitted packets during the interval.

Using the measured success access probability $\tilde{p}_l(t)$, in O-DCF, the transmission length (in mini-slots) is chosen by:

$$\mu_l(t) = \min\left(\frac{\exp(q_l^M(t))}{\tilde{p}_l(t)}, \bar{\mu}\right), \quad (5)$$

where $\bar{\mu}$ is the maximum transmission length (e.g., 64 packets in our setting, which is similar to the maximum aggregation size in 802.11n to ensure the minimum short-term fairness² and prevent channel monopolization by some node). Then, we convert the transmission length in the unit of mini-slots of the 802.11 chipset into that in bytes so as to compute the number of packets for aggregate transmission as follows:

$$\mu_l(\text{bytes}) = \mu_l(\text{slots}) \times c_l(\text{Mb/s}) \times t_{\text{slot}}(\mu\text{s/slot}), \quad (6)$$

where c_l is the link capacity and t_{slot} is the duration of a mini-slot (9 μs in 802.11a). When only a part of μ_l bytes is transmitted due to packetization, we maintain a *deficit counter* to store the remaining bytes of the transmission length that will be used in the next transmission.

3.4 Channel Heterogeneity and Imperfect Sensing

In practice, wireless channels are heterogeneous across users as well as often time-varying. In such environments, most 802.11 hardware exploits multi-rate capability of the PHY layer to adapt their rate, e.g., SampleRate [5]. However, it is known that 802.11 DCF is incapable of utilizing this opportunistic feature, leading to the waste of resource called *performance anomaly* [12]. In other words, 802.11 DCF provides the equal chances to the links (on average), in which case the low-rate links would occupy more time than the high-rate ones, so that the performance degrades. To provide fairness focusing on time shares instead of rate shares, namely *time-fairness* [32], we slightly modify our rules in selecting the initial access probability as well as the transmission length by replacing $\exp(q_l^M(t))$ by $\exp(c_l(t)q_l^M(t))$ in (2) and (5), where $c_l(t)$ is (relative) link capacity of link l at time t , as theoretically verified by [26].

For imperfect sensing cases such as HT and IA scenarios, we also propose to use a virtual carrier sensing via RTS/CTS signaling, as suggested in literature. In O-DCF, unlike in the standard 802.11a/b/g, RTS/CTS signaling is conducted only for the first packet within the transmission length.

4. WHY DOES O-DCF WORK?

4.1 oCSMA Theory

O-DCF is in part motivated by the recent research results on queue-based MAC scheduling in theory community, see e.g., a survey [36] and in particular, the studies

²For measuring short-term fairness, we use the inverse of the largest time difference between two consecutive packet transmissions for a flow.

on oCSMA [15, 22, 23, 25, 27]. oCSMA is characterized as a CSMA that has a specific rule of setting backoff time and transmission length. They are slightly different in terms of the models and conditions, e.g., discrete/continuous, synchronous/asynchronous, or saturated/unsaturated traffic. However, the key idea is largely shared; the queue maintains the demand-supply differential, and the access aggressiveness is controlled by the queue length, which, in turn, depends on the demand (arrival) and the supply (transmission success). It has been proved that as long as $p_l(t) \times \mu_l(t) = \exp(W(q_l(t)))$, where $W(\cdot)$ is a weight function, optimality in terms of throughput or fairness is ensured.

As an example, in the saturated model with infinite backlog, the optimality can be stated as: the long-term rate $\gamma^* = (\gamma_l^* : l \in \mathcal{L})$ (\mathcal{L} is the set of all links) is the solution of the following optimization problem:

$$\max \sum_{l \in \mathcal{L}} U(\gamma_l), \quad \text{such that } \gamma \in \Gamma, \quad (7)$$

where Γ is the throughput region that is the set of all long-term rates possible by any MAC algorithm. It is proved that γ^* can be realizable by any MAC algorithm. Of particular interest is the logarithmic utility function (i.e., $U(\cdot) = \log(\cdot)$), in which case the source rate is controlled by $V/q_l(t)$ for some positive constant V . This source rate control, together with oCSMA, achieves *proportional fairness*, which effectively balances fairness and efficiency.

We highlight that O-DCF is not just a naive implementation of oCSMA, because many assumptions in the oCSMA theory, e.g., no collisions in the continuous time framework, symmetric sensing, perfect channel holding, etc. do not hold in practice. Furthermore, O-DCF is constrained, to be fully compatible with 802.11 chipsets. More importantly, in theory, any combination of p_l and μ_l works if their product is $\exp(W(q_l(t)))$. However, we need a careful combination of them for high performance in practice. All of these issues will be elaborated in the following sections.

Among other results, [24] shows that symmetrically high collision scenarios can induce an excessive aggressiveness by oCSMA flows, which in turn can lead to the complete throughput degradation (e.g., HT). In addition, asymmetric collisions can introduce large disparities in the throughput attained by different flows (e.g., IA). While oCSMA can help with reducing the aggressiveness of advantaged flows, the range of values in which the CW size is adapted is insufficient to provide high performance gains when the transmitters are out of carrier-sense range. Finally, oCSMA excessively prioritizes links with low channel quality, due to queue based aggressiveness control. This introduces severe inefficiency to the performance of oCSMA.

4.2 Tension between Symmetric and Asymmetric Contention

4.2.1 Topological Dependence

A good combination of two CSMA operational parameters for high performance depends on contention topologies.

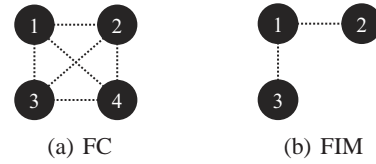


Figure 2: Example topologies' conflicting graphs. Vertices are the links in interference graphs; dotted lines represent interference; (a) FC with 4 links; (b) FIM with 2 outer links.

O-DCF is designed to autonomously choose the combination of access probability and transmission length without explicit knowledge of topological information. We provide our description, assuming that flows are configured in either of the two “extreme” topologies: fully-connected (FC) for symmetric contention and flow-in-the-middle (FIM) for asymmetric contention (see Figure 2). As the name implies, symmetry or asymmetry in contention refers to whether the contention level is similar across flows or not. We use these two topologies just for ease of explanation, and O-DCF generally works well beyond these two topologies.

Recall the two key design ideas of O-DCF: we first choose the initial access probability as a sigmoid function of the queue length and then let it experience BEB. To summarize, BEB is a key component in symmetric contention (see Section 4.2.2) and the sigmoid function based access probability selection is crucial in asymmetric contention (see Section 4.2.3), and both are important in “mixture” topologies (see Section 4.2.4).

4.2.2 O-DCF: How Does Exponential Backoff Help?

In symmetric contention, the access probabilities among the contending flows should be reasonably low; otherwise, throughput will naturally degrade. Note that to guarantee fairness and high (long-term) throughput, a tiny p_l can work as it leads to almost no collision. This is because in that case a significantly long transmission length would recover the long-term throughput, as explained in oCSMA theory. However, such a combination will experience a serious problem in short-term fairness, where a maximum bound on transmission length to guarantee short-term fairness is enforced in practice. For an automatic adaptation to contention level, we utilize BEB as a *fully distributed search process* for the *largest* access probability (i.e., the smallest CW size) that lets the links access in presence of collisions. This usage is in stark contrast to BEB in 802.11 DCF that simply conservatively tries to avoid collisions.

4.2.3 O-DCF: Why Sigmoid Function?

As opposed to symmetric contention, in asymmetric contention such as FIM-like topologies, almost no collision occurs and thus BEB rarely operates (we confirmed in Section 6.2). More importantly, in this case, the starvation of the central flow is a major issue. To tackle this, we require that the CW size (or the access probability) of link l that solely contends with many other links should be *small* (or *high*) and thus *prioritized* enough that the link l avoids rare

channel access and even starvation. To provide such *access differentiation*, we note that the flow in the middle, say l , typically has a more queue buildup than the outer flows. We denote the access probability p_l by some function of queue length q_l , i.e., $p_l = f(q_l)$. Thus, it is natural to design $f(q_l)$ to be *increasing* for access differentiation.

The question is what form of the function $f(q_l)$ is appropriate for high performance. To streamline the exposition, we proceed the discussion with the access probability rather than the CW size. Toward efficient access differentiation, we start by the f 's requirements: for any link l and for $q_{\min} \leq q \leq q_{\max}$,

- R1:** $0 \leq f(q_l) \leq \bar{p} < 1$, where $f(q_{\min}) \approx 0$ and $f(q_{\max}) = \bar{p}$. The largest access probability \bar{p} should be strictly less than one to prevent channel monopolization.
- R2:** $[f(q_l)]_2^3$ should span all the values in $\{1/2^i, i = 0, \dots, 9\}$ each of which corresponds to the CW sizes $\{2^{i+1} - 1, i = 0, \dots, 9\}$ due to the CW granularity constraint **C2**.
- R3:** The transmission lengths of the flows with heavy contention and those with light contention should be similar.

The requirement **R3** is important to prevent the central flow from being starved. In asymmetric contention such as the FIM-like topologies, the flows experiencing heavy contention such as the central one in FIM has very rare chances to access the media. To guarantee (proportional) fairness, it is necessary for such flows to select long transmission lengths whenever holding the channel. However, as mentioned earlier, the maximum transmission length should be bounded for practical purpose such as short-term fairness. This implies that the central flow often needs to stop the transmissions before its required transmission length for optimal fairness is reached. Efficient flow differentiation, which essentially prioritizes the flows with heavy contention in terms of access probability, helps much by reducing the required transmission length with a reasonable value (mostly shorter than the maximum transmission length) towards long-term fairness. An extreme case for asymmetric contention is IA scenario where two flows have asymmetric interference relationship. We will explain in Section 4.3 that our flow differentiation helps a lot in providing (long-term) fairness in such a problematic scenario.

An intuitive way to realize flow differentiation is to set the access probability of link l to be $\exp(q_l)/K$ for some constant K . Then, the rule (5) enforces the transmission length to be around K , *irrespective of the contention levels of the flows* (i.e., **R3**). However, to satisfy **R1**, we use a slightly different function that has a sigmoidal form, $f(q_l) = \frac{\exp(q_l)}{\exp(q_l) + C}$, with some constant C . This function naturally makes the chosen access probability to be strictly less than one for any $q_{\min} \leq q \leq q_{\max}$, unlike $\exp(q_l)/K$, because it is increasing up to $f(q_{\max})$. Clearly, the sigmoid function is not ex-

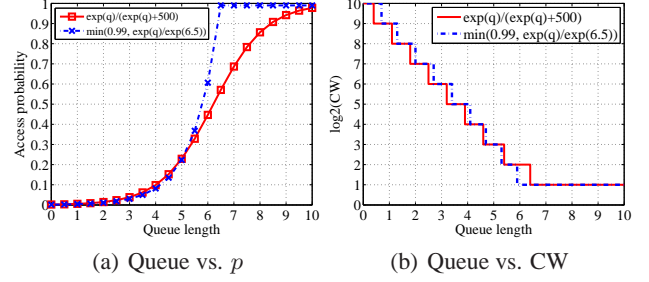


Figure 3: Illustration of sigmoid and exponential functions with respect to queue length.

ponential over the entire $q_{\min} \leq q_l \leq q_{\max}$ values. However, it suffices to have an exponential form up to q'_l with $f(q'_l) = 0.75$, since for a larger $q_l > q'_l$, the CW size approaches one from the CW granularity (but, the access probability is set to be strictly less than one).

Then, the next question is the inflection point, determined by the constant C . We choose C around 500 due to the following reasons. First, for the resultant p to span the whole feasible values (as in **R2**), C should be greater than 500, i.e., $f(q_{\min}) = \frac{\exp(q_{\min})}{\exp(q_{\min}) + 500} \approx \frac{1}{512}$, where $q_{\min} = bQ_{\min} = 0.01$ (see Figure 3(b) in terms of CW). Second, the parameter C determines the location of inflection point in the sigmoid function. For example, let us consider the FIM topology with four outer flows, where the central flow can have its queue length of up to five, while the outer flows have much smaller queue lengths usually less than two. To guarantee the exponential increase in that curve, the x -axis at the inflection point should be larger than five, implying that C larger than 500 is sufficient since $f(5) = \frac{\exp(5)}{\exp(5) + 500} < \frac{1}{2}$. However, too large C values directly results in too long transmission length from (5) because it yields a very low p .

Finally, two remarks are in order: (i) Due to the CW granularity constraint **C2**, the exponential function $f(q_l) = \min(1, \exp(q_l)/\exp(6.5))$ leads to the similar CW mapping to the sigmoid function with $C = 500$, as shown in Figure 3(b). Thus, the sigmoid function may not be a unique choice to satisfy **R1**, **R2**, and **R3**. However, the sigmoid function seems to be more natural, if we consider the possible scenario that the 802.11 chipset allows more choices of CW size than 2^i values. (ii) In theory, the access probability similar to that in (3) has been used in continuous [27] as well as discrete time framework [25], referred to as *Glauber dynamics*. Such a choice of access probability and transmission length is just one of the combinations. However, the access probability in (3) is practically important for high performance, where the choice of C is crucial.

4.2.4 Mixture of Contention Levels

In practice, it is possible for a link to appear in a mixture of topologies with symmetric and asymmetric contention. We study this issue using the example scenarios in Figure 4. First, in Figure 4(a), flow 6 interferes with flows 1, ..., 5 in a fully-connected fashion, and also with flows 7, 8, and 9 in a FIM-like fashion. Since it senses the transmission of

³We denote by $[x]_2$ the $1/2^i$ for some integer i , which is closest to x , e.g., $[0.124]_2 = 1/2^3$ and $i = 3$.

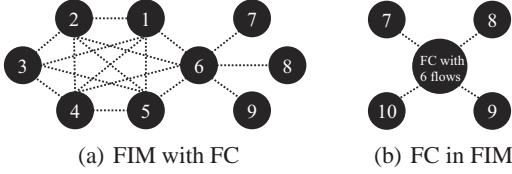


Figure 4: Mixed topologies' conflicting graphs; (a) The flow 6 belongs to both FC and FIM topologies; (b) six flows within a FC group form a FIM topology with four outer flows.

both the remaining links forming the FC group and outer links forming the FIM group, its queue temporarily builds up, thus having a larger access probability than outer links due to the sigmoidal curve. However, it shares the medium equally with others in FC group so that their queue lengths increase together. Thus, in the worst case, BEB can prevent too aggressive access among the links within FC group. More importantly, *even the reduced access probability from BEB is kept larger than those of outer links* (see Section 6.2 for simulation results), thus still being sufficiently prioritized in the FIM topology, preserving proportional fairness. Similar trends are also observed in Figure 4(b).

4.3 Imperfect Sensing and Capture Effect

We have so far explained why O-DCF works with a focus on the case when sensing is perfect. However, in practice, sensing is often *imperfect*, whose cases are discussed under the scenarios, illustrated in Figure 5. Recall that we propose to use the RTS/CTS based virtual sensing in O-DCF. However, the impact of imperfect sensing can still be serious in oCSMA, because of the possible aggravation cycle that collisions increase queue lengths, which in turn leads to more aggressive access and thus heavier collisions, especially under the CW adaptation.

Our queue based initial CW with BEB substantially lessens such bad impacts. In *HT*, if the queue lengths of hidden nodes are large, BEB lets each node increase its CW, so that with small time cost, a transmission succeeds. This successful transmission generally decreases the queue lengths, preventing CW from being too small due to queue based initial CW selection. In *IA*, collisions are asymmetric. Suppose that at some time the advantaged and the disadvantaged flows have small and large queue lengths, respectively. Then, the disadvantaged flow will have a smaller initial CW, thus leading to some successful transmissions and simultaneously the advantaged flows will hear CTS signaling (responding to RTS from the disadvantaged flow) and stop their attempts. This helps a lot in providing fairness between two asymmetric flows. The packet capture effects can be handled by our method similarly to the *IA* scenario, i.e., interference asymmetry. For example, in *HT with capture*, similar behaviors to the *IA* case occur between weak and strong nodes.

5. O-DCF IMPLEMENTATION

5.1 Queue Structure

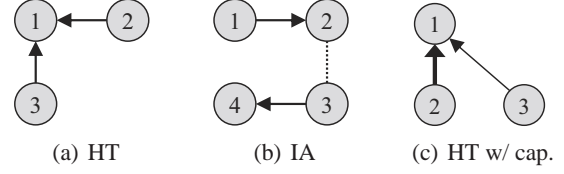


Figure 5: Example topologies of imperfect sensing and packet capture. In network graphs, vertices represent nodes, dotted lines represent connectivity, and arrows represent flows. (a) HT; (b) IA; (c) HT with capture: a thin arrow for weak signal.

We implemented O-DCF through an overlay MAC over legacy 802.11 hardware using our C-based software platform, which requires protocol implementation on top of Mad-WiFi device driver [2]. Due to a limited memory size of legacy network interface card (NIC), we implement CQ and MAQ at the user space level. Note that the scheduling from MAQ to IQ is not an actual packet transmission to the media (*CI*). To minimize the temporal gap between the service from MAQ and the actual transmission, we reduce the buffer limit of IQ to one through a device driver modification.

5.2 O-DCF Scheduler and Parameter Control

A scheduler in O-DCF schedules the packets enqueued at MAQ to send them into the 802.11 hardware, as shown in Figure 1. Whenever IQ in 802.11 becomes empty, the scheduler in O-DCF is notified by a system call such as `raw socket` function and determines the next packet to be enqueued into IQ, by comparing the sizes of multiple per-neighbor MAQs. Meanwhile, the scheduler maintains CSMA parameters, such as CW, AIFS, and NAV values, for each MAQ's HOL packet. To facilitate packet-by-packet parameter control, we piggyback such parameters into the header of HOL packet, so that the modified driver can interpret and set them in the TXQ descriptor of an outgoing packet for the actual transmission.

5.3 Long Data Transmission

When packet aggregation is not supported in legacy 802.11 hardware such as 802.11a/b/g, we take the following approach for consecutive multi-packet transmissions: The O-DCF scheduler assigns different arbitration inter-frame spaces (AIFSs) and CWs for the packets inside the specified transmission length. Since AIFS defines a default interval between packet transmissions and the smallest CW indicates the shortest backoff time, this provides a prioritization for *back-to-back* transmissions until the given transmission length expires. Further, we exploit the network allocation vector (NAV) option that includes the time during which neighbors remain silent irrespective of sensing. This guarantees that even interfering neighbors that cannot sense (due to, e.g., channel fluctuations) do not prevent the transmission during the reserved transmission length. In this way we overcome the constraint on the maximum aggregate frame size (*C4*). RTS/CTS signaling is conducted only for the first packet within the given transmission length. By modifying the device driver, we can turn on or off such a signaling according



(a) Mobile testbed node



(b) FC deployment

Figure 6: Testbed hardware and an example deployment.

to the number of transmitted packets specified by the transmission length.

5.4 Link Capacity Update

As discussed in Section 3.4, to exploit multi-rate capability, we need to get the runtime link capacity information from the device driver. To fetch the runtime capacity, we periodically examine `/proc` filesystem in Linux. The period has some tradeoff between accuracy and overhead. We employ the exponential moving average each second to smooth out the channel variations as well as to avoid too much overhead of reading `/proc` interface.

6. PERFORMANCE EVALUATION

6.1 Hardware Testbed

Setup. To evaluate O-DCF’s performance, we use both GloMoSim [1] based simulation and real experiment on a 16-node wireless multihop testbed. In the testbed, each node runs on Linux kernel 2.6.31 and is a netbook platform (1.66 GHz CPU and 1 GB RAM) equipped with a single 802.11a/b/g NIC (Atheros AR5006 chipset), as shown in Figure 6. We built our O-DCF on top of legacy 802.11 hardware, and modified the MadWiFi driver for O-DCF’s operations. To avoid external interference, we select a 5.805 GHz band in 802.11a. Also we set the MAC retry limit to four. The default link capacity is fixed with 6 Mb/s, but we vary the capacity or turn on auto rate adjustment for the evaluation of the heterogeneous channel cases. For all tested scenarios, we repeat ten times (each lasting for 100 seconds) and measure the goodput received at the flow’s destination. The length of error bars in all plots represents standard deviation. The packet size is set to be 1000 bytes. We choose the $b = 0.01$ in Section 3.1, and the lower and upper bounds for MAQ as $Q_{\min} = 1$ and $Q_{\max} = 1000$, which, however, we observe, does not significantly impact the results and the trends in all of the results.

Tested protocols. We compare the following algorithms: (i) 802.11 DCF, (ii) standard oCSMA, and (iii) DiffQ [34]. For the standard oCSMA algorithm, we implement two practical versions: (i) *CW adaptation* in which we typically fix the transmission length μ with a single packet (in our case, 1000 bytes is used and corresponds to about 150 mini-slots in 802.11a at 6 Mb/s rate) and control the access probability $p_l(t)$, such that $p_l(t) \times \mu = \exp(q_l(t))$, as used in the oCSMA evaluation research [24], and (ii) μ adaptation with

Table 1: Simulation (up) and experiment (down). Aggregate throughput in FC topology for 3, 6, 9, 12 flows

N	802.11	DiffQ	CW adapt.	μ adapt.	O-DCF
3	4235	4311	4423	4259	4700
6	3849	4042	1321	4566	4859
9	3616	2826	1151	4765	4530
12	3513	1189	116	4814	4501

N	802.11	DiffQ	CW adapt.	μ adapt.	O-DCF
3	4472	4719	4541	4469	4843
6	4119	4585	2186	4457	4664
9	4126	4296	2362	4789	4680
12	4134	4055	2373	4849	4794

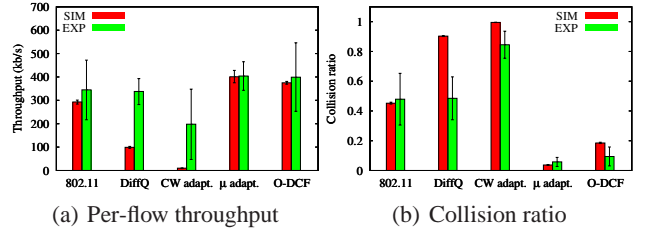


Figure 7: Performance comparison among tested algorithms in FC topology with 12 flows.

BEB (simply, μ adaptation) in which we delegate the selection of $p_l(t)$ to 802.11 DCF and control $\mu_l(t) = \exp(q_l(t))/p$. Thus, CW starts from $CW_{\min} = 15$ slots in 802.11a and doubles per each collision. DiffQ is a *heuristic* queue-based algorithm using 802.11e feature and schedules the interfering links with different priorities based on queue lengths. Although it shares the philosophy of fair channel access by granting more chances to less served links with oCSMA and O-DCF, it adapts using several heuristics, thus guaranteeing suboptimal performance, which makes a difference from oCSMA (under ideal condition) and O-DCF (even in practice). To be consistent, all the protocols evaluated in our testbed are implemented under 802.11 constraint and thus they keep intrinsic features such as BEB⁴.

Metrics. For simple topologies, we directly compute the optimal rate allocations in terms of proportional fairness and compare it with the results of the tested algorithms. In more large-scale scenarios, it is hard to benchmark the optimal results. Thus, we use the following method: for n flows and average per-flow throughput $\gamma_i, 1 \leq i \leq n$, we define (i) sum of log utility for efficiency, i.e., $\sum_{i=1}^n \log(\gamma_i)$, and (ii) Jain’s index for fairness, i.e., $(\sum_{i=1}^n \gamma_i)^2 / (n \sum_{i=1}^n \gamma_i^2)$ [14].

6.2 Fully-connected, FIM, and Mixture

Fully-connected: Impact of contention degrees. We first examine the FC topologies with varying the number of contending flows (see Figure 2(a)). Table 1 summarizes the aggregate throughputs both in simulation and experiment. O-DCF outperforms 802.11 DCF, DiffQ, and CW adaptation regardless of the contention levels. This is mainly due to O-

⁴In literature, e.g., [29], BEB is known to be disabled by using TXQ descriptor in the device driver, which however does not work in our chipset. We confirmed this via kernel level measurement.

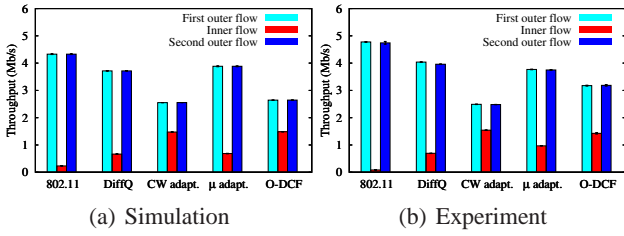


Figure 8: Performance comparison among tested algorithms in FIM topology with two outer flows.

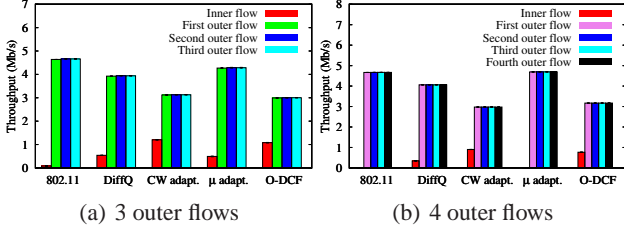


Figure 9: Simulation. Throughput comparison among tested algorithms in FIM topology with three and four outer flows.

DCF’s adaptivity to the contention levels with BEB and the enlarged transmission length driven by the queue lengths. CW adaptation and DiffQ perform poorly, because as the number of contending flows increases, they have more performance loss, where more collisions lead to more aggressive access, and thus much more collisions in a vicious cycle. In 802.11, all nodes start contending with a fixed but aggressive CW value, thus experiencing quite many collisions despite BEB operation (see Figure 7).

O-DCF shows a little lower throughput than μ adaptation. It sometimes has a smaller CW than μ adaptation, causing more collisions when there are many contending flows. However, such a difference in CW values makes a big difference of short-term fairness performance. For example, in FC with 12 flows, we measured the largest inter-TX time of a flow under two schemes: 3.75s vs. 7.26s for O-DCF and μ adaptation, respectively. This can be explained by the corresponding transmission length; O-DCF requires much smaller (thus practical) transmission length (almost less than 20 packets), while μ adaptation requires much longer (thus impractical) transmission length that is often upper bounded by the maximum length (i.e., 64 packets in our setting). We confirm that there is a tradeoff between long-term efficiency and short-term fairness even in practice.

We comment that DiffQ and CW adaptation in experiment perform better than that in simulation, because in experiment, BEB is played (C3) more than its original design (in fact, no BEB operation is allowed in CW adaptation), which actually shows the power of BEB as a distributed tuning of CW. This is supported by the fact that 802.11, which has BEB in itself, also performs reasonably well. The performance difference between experiment and simulation also comes from the capture effect in experiment in the deployment of nodes in close proximity as shown in Figure 6(b).

FIM: Impact of contention asymmetry. Next, we study the case of asymmetric contention, using the FIM topology (see

Figure 2(b)). In this case, it is well-known that the central flow experiences serious starvation [8, 9, 34] in 802.11 DCF, as also shown in Figure 8. As mentioned earlier before, we observe that collisions are rare (less than 10%⁵ in simulation, less than 2% in experiment). In contrast to the FC cases, BEB does not operate frequently in experiment, and thus the performance results are very similar in simulation and experiment.

A main property to verify is whether an algorithm achieves proportional-fair (PF) or not. We can see that O-DCF almost achieves PF exactly, where 2:1:2 is the optimal throughput ratio under PF in FIM with two outer flows. This is due to the efficient access differentiation caused by our queue based initial CW selection. As expected, 802.11’s starvation of the central flow is the most serious. DiffQ resolves the starvation of the central flow well, but it shows suboptimal performance due to the heuristic setting of CW size. We see that CW adaptation is also good in fairness, because in presence of few collisions, CW adaptation also has an adaptive feature of adjusting CW to the queue lengths. However, in μ adaptation, there still exists a lack of fairness between the central and outer flows, because the CW size is fixed with a small value, similarly to 802.11 and thus the outer flows have more power to grab the channel. On the other hand, the central flow needs a longer transmission length once it grabs the channel. This extended transmission of the inner flow leads to the queue buildup of outer flows, which, in turn, makes outer flows access the channel more aggressively. This unfairness is amplified as the number of outer flows increases, as shown in Figure 9, where we only plot the simulation results since the topologies cannot be easily produced in a hardware testbed.

Mixture: Impact of combination of topological features. We perform simulations to study how O-DCF works in the topology with a mixture of FC and FIM, as shown in Figure 4. Earlier, we mentioned that two features (BEB and queue-based initial CW selection) *may* conflict with each other. Now we will show that it actually does not here.

Figure 10(a) shows the normalized per-flow throughput by the optimal one (i.e., PF share) over the topology in Figure 4(a). We observe that O-DCF outperforms others in terms of fairness. The reason is explained as follows: Suppose that flow 6 is fully-connected with flows 1-5. Then, its access probability will be set to be some value, say p_6 , so that collisions are more or less minimized. However, in Figure 4(a), flow 6 should have a high access probability to be prioritized over flows 7-9. A desirable solution would be to make flow 6’s probability higher than p_6 (for prioritization considering the FIM part), as well as flows 1-5’s probabilities lower than that in the case of only FC (for collision reduction). This is indeed achieved by our queue-length based initial CW selection with BEB in a distributed manner, ver-

⁵This seems quite high, but the reason is that the total number of TX attempts at central flow is small. Thus, the absolute number of collisions is small.

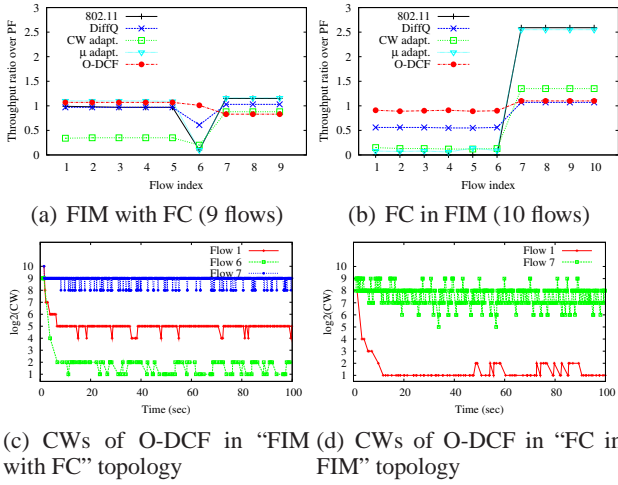


Figure 10: Simulation. (a)-(b): Performance comparison among tested algorithms in two mixed topologies; the flow indexes are the same as in Figure 4; we plot the throughput ratio over optimality: the closer to one the ratio is, the better fairness is; (c)-(d): CW traces of representative flows are plotted over time in O-DCF.

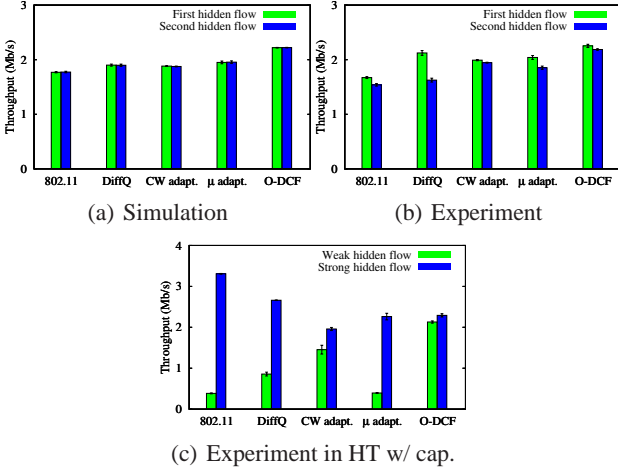


Figure 11: Throughput comparison among tested algorithms in HT topology w/o (up) and w/ packet capture (down).

ified by Figure 10(c). Clearly, flows 1-5 need longer transmission lengths (and thus hurting short-term fairness). They turn out not to be impractically long in the scenario considered here. Similar principles are applied to the topology in Figure 4(b), whose CW traces are shown in Figure 10(b).

6.3 Imperfect Sensing and Capture Effect

We now investigate the impact of imperfect sensing in O-DCF with the topologies: HT, IA, and HT with capture, which are depicted in Figure 5. As discussed in Section 4.3, we enable a virtual sensing, i.e., RTS/CTS signaling by default for better channel reservation before data transmission in all tested algorithms.

Figures 11 and 12 show the throughput results for HT and IA, respectively. First, in HT, O-DCF outperforms others in symmetric interference conditions by hidden nodes, as well as asymmetric conditions due to packet capture. Par-

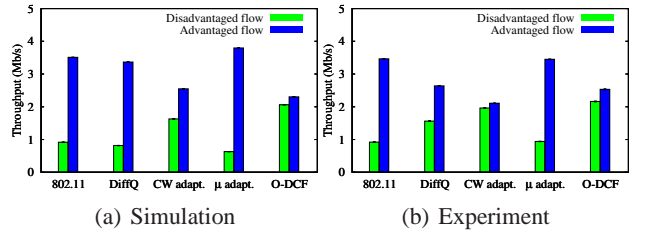


Figure 12: Throughput comparison among tested algorithms in IA topology.

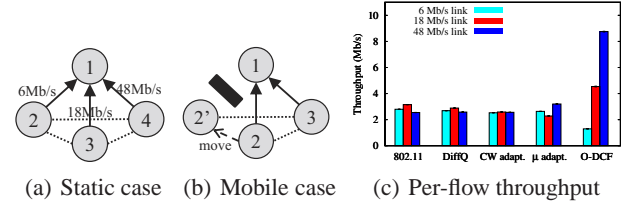


Figure 13: Experiment. Single-hop network scenario consisting of clients and one AP; (a) static case: all nodes remain fixed with different PHY rates; (b) mobile case: node 2 moves away from node 1 at 60 seconds.

ticularly, in O-DCF, collisions and thus BEB allow the hidden flows to access the media with larger CWs (i.e., less aggressiveness), resulting in many successful RTS/CTS exchanges. Fairness is guaranteed by the transmission length control. Second, in IA, our O-DCF shows very fair and high throughput, where the advantaged flow has a larger CW due to small backlogs, and the disadvantaged flow also uses a larger CW due to BEB, responding well to collisions. As a result, both flows contend with sufficiently large CW values without heavy collisions, enjoying better RTS/CTS-based reservation. Similarly, we can ensure fairness in the scenario with packet capture. Note that μ adaptation performs badly especially under asymmetric contention such as HT with capture and IA topologies. Similarly to 802.11 DCF, its fixed CW value makes BEB happen frequently, hindering channel access of the weak hidden node in HT with capture or the disadvantaged node in IA. DiffQ performs similarly due to the still aggressive setting of CW values. However, CW adaptation grants more aggressiveness to less-served flows, thus reducing the throughput gap between the two flows in both scenarios, while still leaving a small gap from optimality.

6.4 Heterogeneous Channels

We analyze O-DCF's performance for the heterogeneous channel conditions configured by the topology of Figures 13(a) and 13(b). We consider two scenarios: (i) *static*: nodes are stationary with different link rates, 6, 18, and 48 Mb/s, and (ii) *mobile*: each node turns on the auto-rate functionality and two clients send their data to a single AP, and after 60 seconds, one of two clients (say node 2) moves away from AP (node 1). In adapting the rate, we employ the SampleRate algorithm [5], popularly used in MadWiFi driver. We measure the runtime PHY rate information updated every one second interval, as mentioned in Section 5.4.

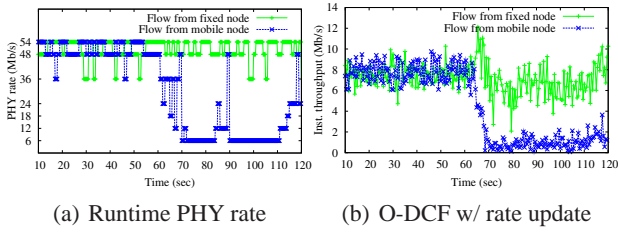


Figure 14: Experiment. Performance evaluation in mobile scenario (Figure 13(b)).

First, in the static scenario, Figure 13(c) shows the average per-flow throughput. We observe that only O-DCF can attain proportional fair rate allocation in an efficient manner, because of the consideration of the different link rates in the choice of CWs and transmission lengths, whereas the other protocols show severe inefficiency that the flows with higher rates are significantly penalized by the flow with lower rate. In addition to the long-term fairness study in the static scenario, we examine the responsiveness of O-DCF to channel variations in the mobile scenario. The mobile node’s movement affects its channel conditions, as shown in Figure 14(a). We trace the instantaneous throughput of both fixed and mobile nodes in Figure 14(b), where we see that the incorporation of the runtime PHY rate in O-DCF indeed helps in achieving throughput efficiency instantaneously even in the auto-rate enabled environment.

6.5 Experiment in Random Topology

We have so far focused on simple topologies representing their unique features in terms of contention and sensing situation. We now perform more general experiments using a 16-node testbed topology, as shown in Figure 15(a). We compare five algorithms in the network with five and seven concurrent flows. Using this random topology, we evaluate the impact of mixed problems, such as hidden terminals and heavy contention scenarios including FIM scenario.

Figure 15(b) compares Jain’s fairness achieved by all the algorithms for two scenarios. We find that over all the scenarios, O-DCF outperforms others in terms of fairness (up to 87.1% over 802.11 DCF and 30.3% over DiffQ), while its sum utility is similar with others. The fairness gain can be manifested in the distribution of per-flow throughput, as shown in Figures 15(c) and 15(d). O-DCF effectively prioritizes the flows with more contention degree (e.g., flow 10 \rightarrow 9 forms *flow-in-the-middle* with flows 7 \rightarrow 8 and 15 \rightarrow 14) and provides enough transmission chances to highly interfered flows (i.e., 8 \rightarrow 9, 10 \rightarrow 13, and 14 \rightarrow 13), compared to 802.11 DCF and DiffQ. The experimental topology is somewhat limited in size due to physical structure of our building, so that the topology is close to be fully-connected, leading to a small performance gap between oCSMA and O-DCF. On the other hand, 802.11 DCF yields severe throughput disparities of more than 40 times between flows 12 \rightarrow 11 and 10 \rightarrow 13 in the second scenario. Compared to 802.11 DCF, DiffQ performs fairly well in the sense that it prioritizes highly interfered flows. However, its access prioritization is heuristic, so there is still room for improvement toward optimality where compared to O-DCF.

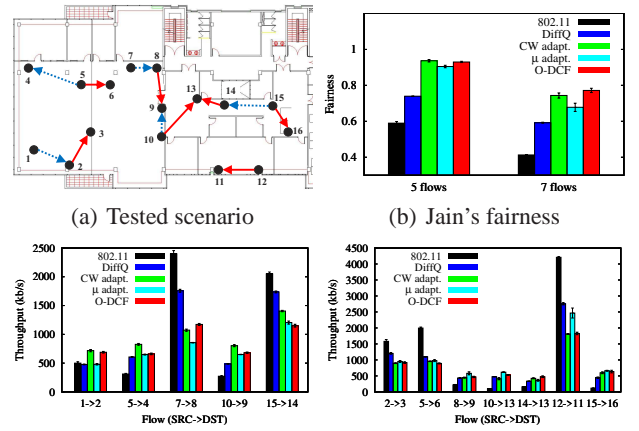


Figure 15: Experiment. Tested topology and performance comparison; (a) 16 nodes denoted by triangles are distributed in the area of 40m x 20m; dotted (solid) arrows represent 5 (7) flows for the first (second) scenario. (b) Jain’s fairness comparison among tested algorithms. (c)-(d) Per-flow throughput distributions.

Figure 15(c) shows the per-flow throughput of 5 flows. O-DCF effectively prioritizes the flows with more contention degree (e.g., flow 10 \rightarrow 9 forms *flow-in-the-middle* with flows 7 \rightarrow 8 and 15 \rightarrow 14) and provides enough transmission chances to highly interfered flows (i.e., 8 \rightarrow 9, 10 \rightarrow 13, and 14 \rightarrow 13), compared to 802.11 DCF and DiffQ. The experimental topology is somewhat limited in size due to physical structure of our building, so that the topology is close to be fully-connected, leading to a small performance gap between oCSMA and O-DCF. On the other hand, 802.11 DCF yields severe throughput disparities of more than 40 times between flows 12 \rightarrow 11 and 10 \rightarrow 13 in the second scenario. Compared to 802.11 DCF, DiffQ performs fairly well in the sense that it prioritizes highly interfered flows. However, its access prioritization is heuristic, so there is still room for improvement toward optimality where compared to O-DCF.

6.6 Simulation in Large Topologies

Finally, we extend the evaluation of O-DCF to two large-scale scenarios in a wider area. The first is a grid network where 16 nodes are apart from each other with 250m, and the second is a random network where 30 nodes are deployed randomly within an area of 1000m \times 1000m. These networks, depicted in Figures 16(a) and 16(b), contain a mixture of the previously discussed problematic scenarios, such as HT, IA, and FIM, as well as highly interfering FC groups. For a given number of flows, we construct 10 scenarios with different random single-hop flows. In particular, we simulate 6 and 12 flows over grid and random networks, respectively.

Figure 16(c) compares the Jain’s fairness achieved by five algorithms. O-DCF enhances fairness up to 41.0% (resp., 29.9%) over 802.11 DCF and 24.0% (resp., 12.6%) over DiffQ in the random (resp., grid) network. Compared to the previous experiments, we observe more throughput disparities of contending flows under DiffQ and μ adaptation. In most scenarios, randomly chosen flows likely have problematic relationships such as HT and IA. This leads to lower fairness of DiffQ and μ adaptation than O-DCF and CW adaptation, since they are vulnerable to imperfect sensing scenarios, as examined in Section 6.3. Moreover, O-DCF experiences much less collisions than CW adaptation, thus leading to better throughput. Finally, our O-DCF consistently shows a slightly better performance in terms of sum utility (see Figure 16(d)).

7. CONCLUSION

We presented O-DCF so that 802.11 can work close to optimal in practice. The major design issues to make 802.11

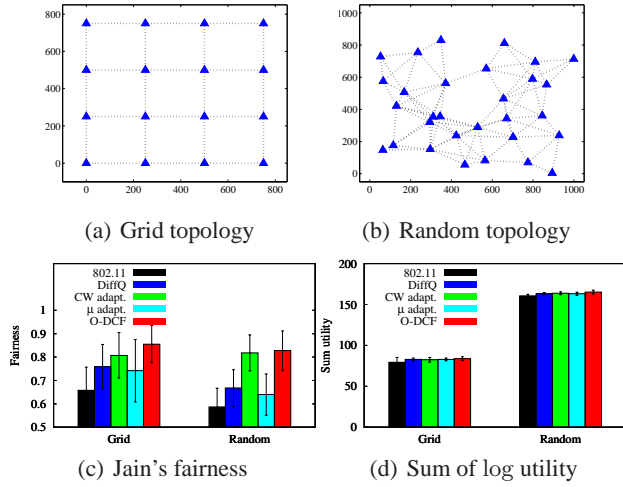


Figure 16: Simulation. Large-scale topologies within 1000m × 1000m area and each node denoted by triangles has transmission and sensing ranges equal to 280m; (a) 16 nodes form a grid network; (b) 30 nodes are deployed randomly; (c)-(d) fairness and sum utility comparison among tested algorithms.

DCF optimal include contention window selection and transmission length control against network contention, imperfect sensing, channel heterogeneity, packet capture without any message passing. Moreover, our proposed O-DCF can be implemented with simple software modifications on top of legacy 802.11 hardware. Through extensive simulations and experiments using 16-node wireless testbed, we have demonstrated that O-DCF performs similarly to that in theory, and outperforms other MAC protocols, such as oCSMA, 802.11 DCF, and DiffQ, under a wide range of scenarios. Among the vast literature on 802.11/CSMA, O-DCF seems to be the first one that is validated through hardware experiments to be both near-optimal in utility maximization's efficiency and fairness metrics and 802.11 legacy-compatible.

8. REFERENCES

- [1] GloMoSim. <http://pcl.cs.ucla.edu/projects/gloimosim/>.
- [2] Multiband Atheros Driver for WiFi. <http://madwifi-project.org/>.
- [3] A. Aziz, D. Starobinski, P. Thiran, and A. Fawal. EZ-Flow: Removing turbulence in IEEE 802.11 wireless mesh networks without message passing. In *Proc. ACM CoNEXT*, 2009.
- [4] V. Bharghavan, A. Demers, S. Shenker, and L. Zhang. MACAW: A media access protocol for wireless LANs. In *Proc. ACM SIGCOMM*, 1994.
- [5] J. C. Bicket. Bit-rate selection in wireless networks. Master's thesis, MIT, 2005.
- [6] T. Bonald and M. Feuillet. On flow-aware CSMA in multi-channel wireless networks. In *Proc. CISS*, 2011.
- [7] F. Cali, M. Conti, and E. Gregori. Dynamic tuning of the IEEE 802.11 protocol to achieve a theoretical throughput limit. *IEEE/ACM Trans. Netw.*, 8(6):785–799, Dec. 2000.
- [8] W. Chen, Y. Wang, M. Chen, and S. C. Liew. On the performance of TCP over throughput-optimal CSMA. In *Proc. IEEE IWQoS*, 2011.
- [9] M. Garetto, T. Salonidis, and E. Knightly. Modeling per-flow throughput and capturing starvation in CSMA multi-hop wireless networks. In *Proc. IEEE INFOCOM*, 2006.
- [10] Y. Grunenberger, M. Heusse, F. Rousseau, and A. Duda. Experience with an implementation of the idle sense wireless access method. In *Proc. ACM CoNEXT*, 2007.
- [11] S.-J. Han, T. Nandagopal, Y. Bejerano, and H.-G. Choi. Analysis of spatial unfairness in wireless LANs. In *Proc. IEEE INFOCOM*, 2009.
- [12] M. Heusse, F. Rousseau, G. Berger-Sabbatel, and A. Duda. Performance anomaly of 802.11b. In *Proc. IEEE INFOCOM*, 2003.
- [13] M. Heusse, F. Rousseau, R. Guillier, and A. Duda. Idle Sense: an optimal access method for high throughput and fairness in rate diverse wireless LANs. In *Proc. ACM SIGCOMM*, 2005.
- [14] R. K. Jain, D. W. Chiu, and W. R. Hawe. A quantitative measure of fairness and discrimination for resource allocation in shared computer systems. *DEC-TR-301*, 1984.
- [15] L. Jiang and J. Walrand. A distributed CSMA algorithm for throughput and utility maximization in wireless networks. *IEEE/ACM Trans. Netw.*, 18(3):960–972, Jun. 2010.
- [16] W. Kim, H. K. Wright, and S. M. Nettles. Improving the performance of multi-hop wireless networks using frame aggregation and broadcast for TCP ACKs. In *Proc. ACM CoNEXT*, 2008.
- [17] Y. Kim, S. Choi, K. Jang, and H. Hwang. Throughput enhancement of IEEE 802.11 WLAN via frame aggregation. In *Proc. VTC-Fall*, 2004.
- [18] R. Laufer, T. Salonidis, H. Lundgren, and P. L. Guyader. XPRESS: A cross-layer backpressure architecture for wireless multi-hop networks. In *Proc. ACM MobiCom*, 2011.
- [19] J. Lee, H.-W. Lee, Y. Yi, and S. Chong. Improving TCP performance over optimal CSMA in wireless multi-hop networks. To appear in *IEEE Comm. Let.*, 2012.
- [20] J. Lee, J. Lee, Y. Yi, S. Chong, A. Proutiere, and M. Chiang. Implementing utility-optimal CSMA. In *Proc. Allerton Conf.*, 2009.
- [21] T. Li, M. K. Han, A. Bhartia, L. Qiu, E. Rozner, Y. Zhang, and B. Zarikoff. CRMA: collision-resistant multiple access. In *Proc. ACM MobiCom*, 2011.
- [22] J. Liu, Y. Yi, A. Proutiere, M. Chiang, and H. V. Poor. Towards utility-optimal random access without message passing. *Wirel. Commu. Mob. Comp.*, 10(1):115–128, Jan. 2010.
- [23] P. Marbach and A. Eryilmaz. A backlog-based CSMA mechanism to achieve fairness and throughput-optimality in multihop wireless networks. In *Proc. Allerton Conf.*, 2008.
- [24] B. Nardelli, J. Lee, K. Lee, Y. Yi, S. Chong, E. Knightly, and M. Chiang. Experimental evaluation of optimal CSMA. In *Proc. IEEE INFOCOM*, 2011.
- [25] J. Ni, B. Tan, and R. Srikant. Q-CSMA: Queue-length based CSMA/CA algorithms for achieving maximum throughput and low delay in wireless networks. In *Proc. IEEE INFOCOM*, 2010.
- [26] A. Proutiere, Y. Yi, T. Lan, and M. Chiang. Resource allocation over network dynamics without timescale separation. In *Proc. IEEE INFOCOM*, 2010.
- [27] S. Rajagopalan, D. Shah, and J. Shin. Network adiabatic theorem: An efficient randomized protocol for contention resolution. In *Proc. ACM SIGMETRICS*, 2009.
- [28] S. Sen, R. R. Choudhury, and S. Nelakuditi. CSMA/CN: carrier sense multiple access with collision notification. In *Proc. ACM MobiCom*, 2010.
- [29] A. Sharma and E. M. Belding. FreeMAC: framework for multi-channel mac development on 802.11 hardware. In *Proc. ACM PRESTO*, 2008.
- [30] V. A. Siris and G. Stamatakis. Optimal CWmin selection for achieving proportional fairness in multi-rate 802.11e WLANs: test-bed implementation and evaluation. In *Proc.*

- ACM WinTECH*, 2006.
- [31] D. Skordoulis, Q. Ni, H.-H. Chen, A. P. Stephens, C. Liu, and A. Jamalipour. IEEE 802.11n MAC Frame Aggregation Mechanisms for Next-Generation High-Throughput WLANs. *IEEE Wirel. Comm.*, 15(1):40–47, Feb. 2008.
 - [32] G. Tan and J. Gutttag. Time-based fairness improves performance in multi-rate wireless LANs. In *Proc. USENIX*, 2004.
 - [33] X. Wang and K. Kar. Throughput modelling and fairness issues in CSMA/CA based ad-hoc networks. In *Proc. IEEE INFOCOM*, 2005.
 - [34] A. Warrior, S. Janakiraman, S. Ha, and I. Rhee. DiffQ: Practical differential backlog congestion control for wireless networks. In *Proc. IEEE INFOCOM*, 2009.
 - [35] H. Wu, Y. Peng, K. Long, S. Cheng, and J. Ma. Performance of reliable transport protocol over IEEE 802.11 wireless LAN: Analysis and enhancement. In *Proc. IEEE INFOCOM*, 2002.
 - [36] Y. Yi and M. Chiang. *Next-Generation Internet Architectures and Protocols*. Cambridge University Press, 2011. Chapter 9: Stochastic network utility maximization and wireless scheduling.